Electronic Supplementary Information

Designed assembly of porous cobalt oxide/carbon nanotentacles on electrospun hollow carbon nanofibers network for supercapacitor

Tanka Mukhiya [a, b], Gunendra Prasad Ojha [a], Bipeen Dahal [a, c], Taewoo Kim [a], Kisan Chhetri [a], Minju Lee [a], Su-Hyeong Chae [a], Alagan Muthurasu [a], Arjun Prasad Tiwari [a, d], Hak Yong Kim [a, e]*

[a]Department of BIN Convergence Technology, Jeonbuk National University, Jeonju 561-756, Republic of Korea

[b]Department of Chemistry, Bhaktapur Multiple Campus, Tribhuvan University, Nepal

[c]Central Department of Chemistry, Tribhuvan University, Nepal

[d]Carbon Nano Convergence Technology Center for Next Generation Engineers (CNN), Jeonbuk National University, Jeonju 561-756, Republic of Korea

[e]Department of Organic Materials and Fiber Engineering, Jeonbuk National University, Jeonju 561-756, Republic of Korea

*Corresponding author. Tel: +82-10-4902-6300. E-mail: khy@jbnu.ac.kr (H.-Y. Kim)

Calculation for electrochemical parameters;

The specfic capacity of pseudocapacitive electrode material in three electrode electrochemical cell was calculated from GCD curve using the equation;

$$C = \frac{2I \times \int V dt_d \times 1000}{m \times V \times 60 \times 60} \quad (1)$$

where, C is the specific capacity (mA h g^{-1}), I is the constant discharge current (A), t_d is the discharging time (s), V is the voltage difference in discharge (V), $\int V dt_d$ is the integral area of the discharge curve and m is the mass of the active electrode material (g).

To assemble the asymmetric supercapacitor device (ASC), optimal mass ratio of electrode materials was calculated using equation (2).

$$\frac{m_+}{m_-} = \frac{C_- \times V_-}{C_+ \times V_+} \quad (2)$$

where C_+, C_-, m_+, m_-, V_+, and V_- are specific capacity (mA h g^{-1}), mass (g) and potential window (V) of positive and negative electrodes respectively. After preparation, electrodes were soaked into 2 M aqueous KOH electrolyte and assembled in a coin cell device using cellulose paper separator (NKK, Nippon, Kodoshi Corporation). The performance of the device was evaluated using the following equations;

$$E = \frac{I \times \int V dt_d \times 1000}{m \times 60 \times 60} \quad (3)$$

$$P = \frac{E \times 60 \times 60}{t_d} \quad (4)$$

$$n = \frac{t_d}{t_c} \quad (5)$$

where t_c is the charging time (s), E is the energy density (W h kg^{-1}), P is the power density (W kg^{-1}) and n is the Coulombic efficiency of the assembled ASC device.

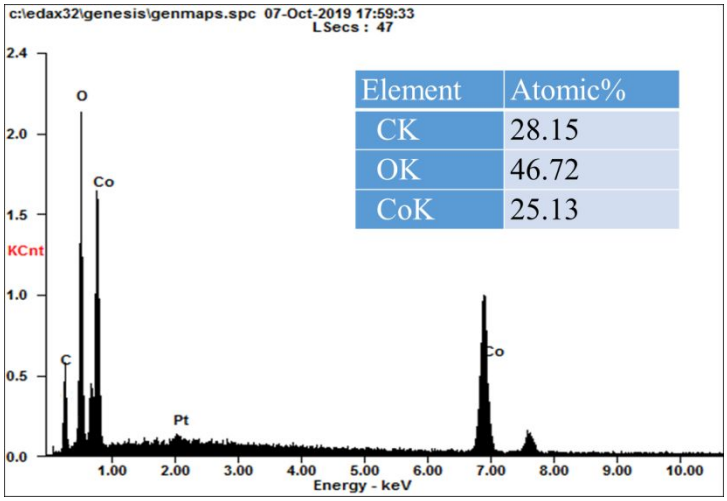

Fig. S1 EDX spectrum of 3D Co_3O_4/C@HCNFs nanocomposite

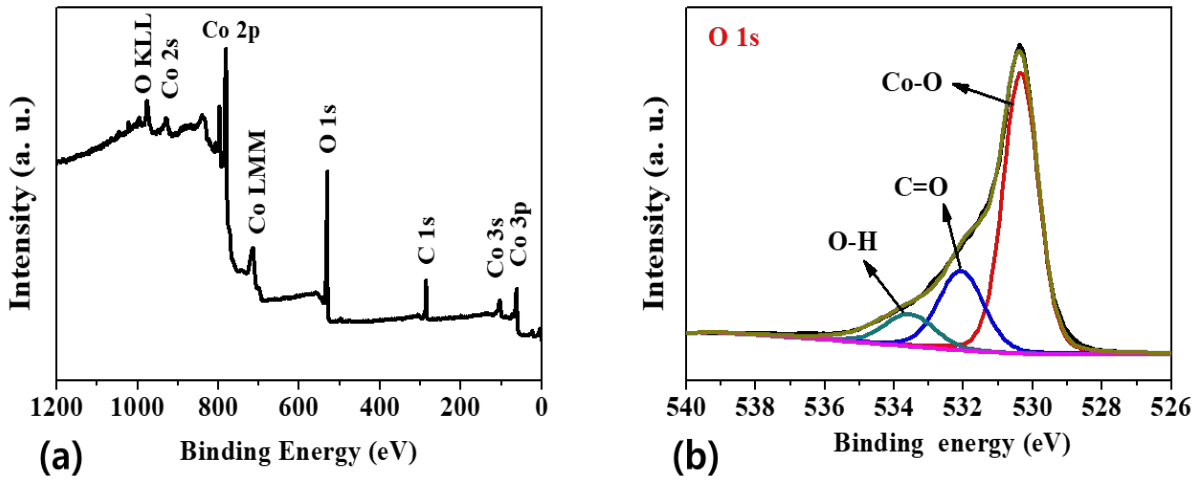

Fig. S2 XPS spectra of 3D Co_3O_4/C@HCNFs nanocomposite; (a) Survey spectrum and (b) High resolution spectrum of O 1s

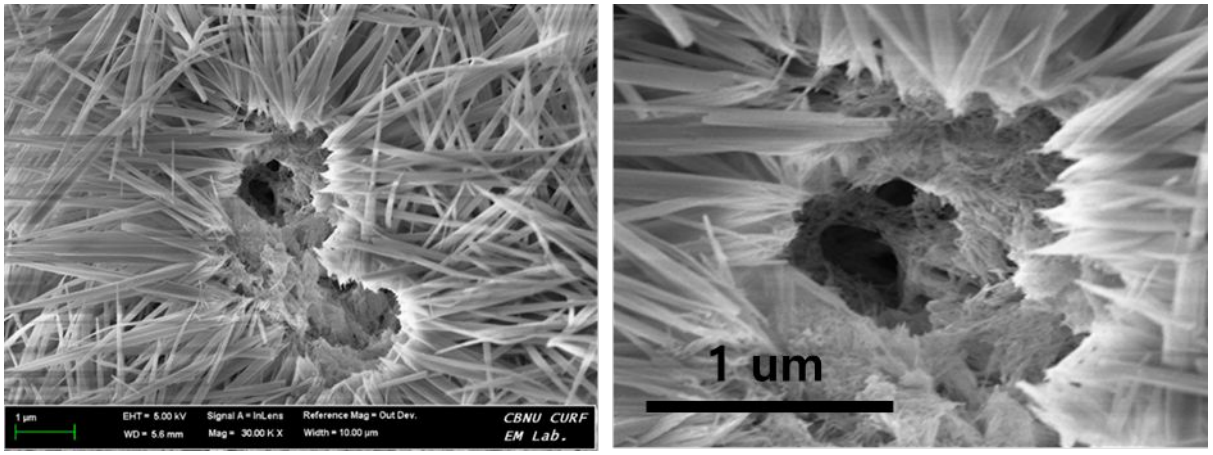

Fig. S3 Cross sectional view of 3D $Co(CO_3)_{0.5}OH.0.11H_2O$@HCNFs

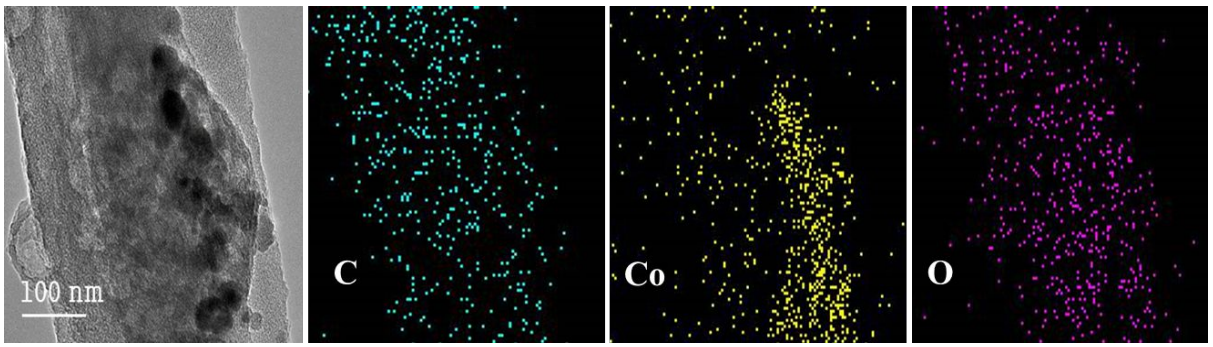

Fig. S4 Elemental mapping of HCNFs in the 3D Co_3O_4/C@HCNFs nanocomposite

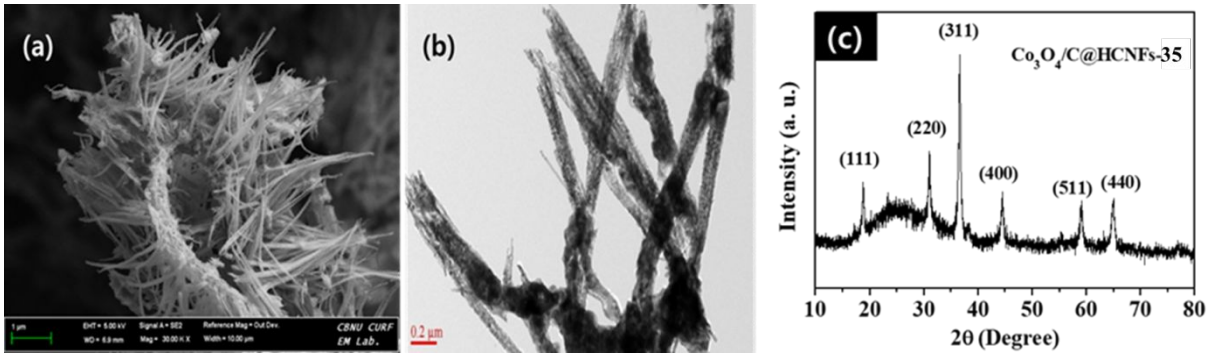

Fig. S5 3D Co_3O_4/C@HCNFs-35 nanocomposite; (a) FE-SEM image, (b) TEM image and (c) XRD pattern

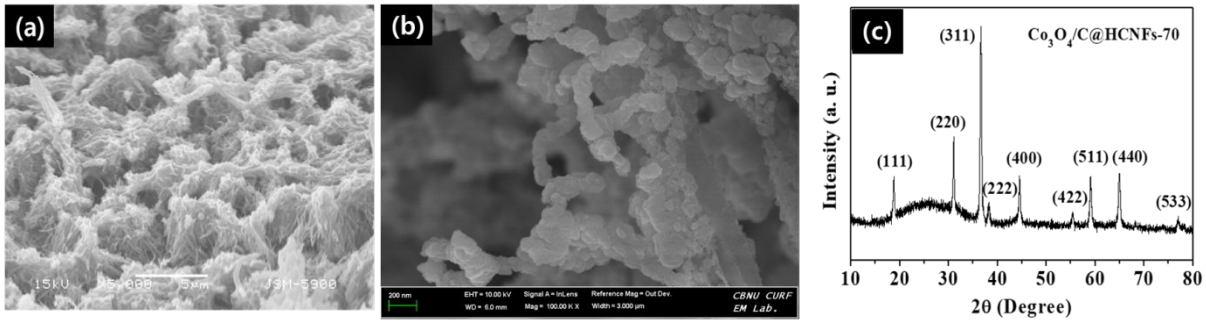

Fig. S6 3D Co_3O_4/C@HCNFs-70 nanocomposite; (a) SEM image, (b) FE-SEM image and (c) XRD pattern

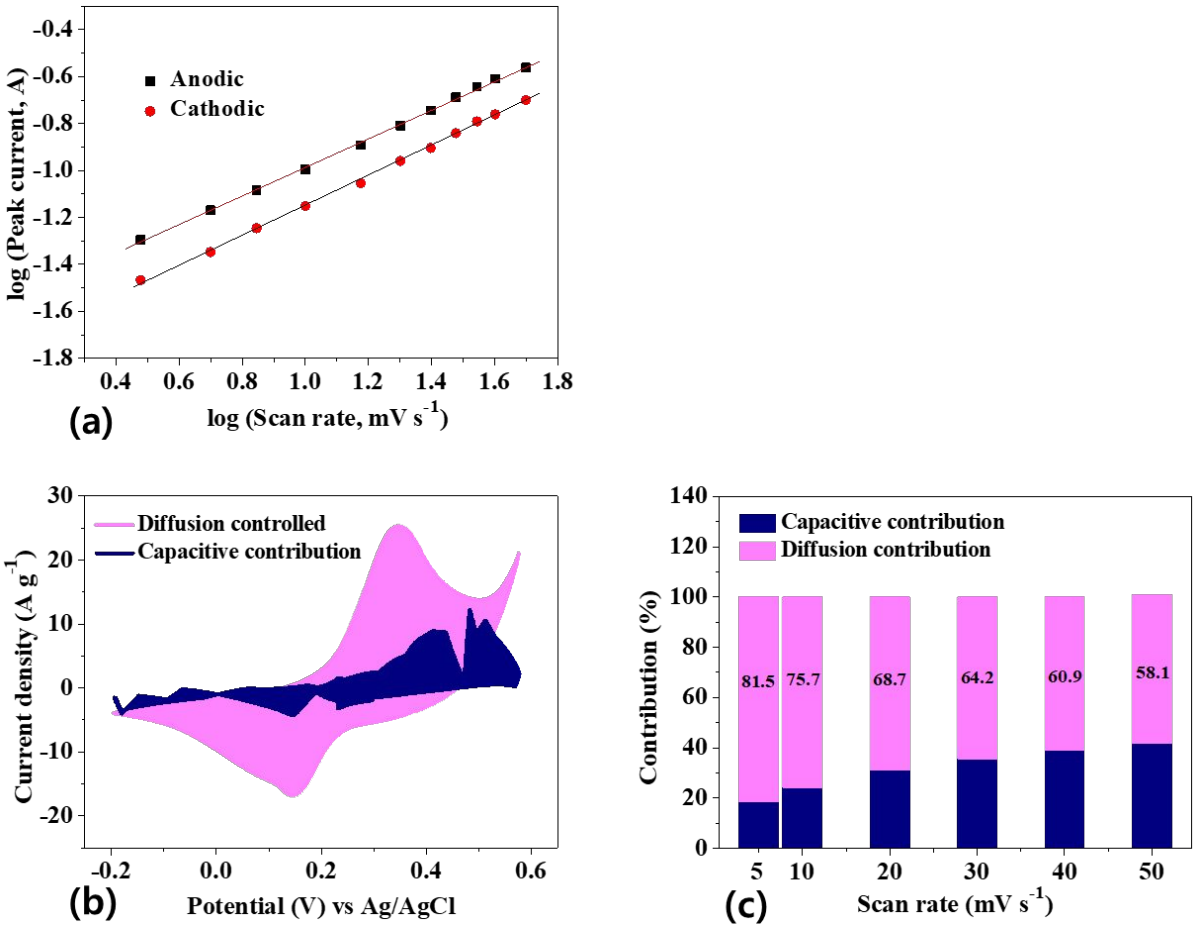

Fig. S7 Plot of log (i) vs log v of 3D Co_3O_4/C@HCNFs, (b) Separation of capacitive and diffusion controlled current at 10 mV s^{-1} and (c) Relative contribution of capacitive and diffusion processes in the charge storage at different scan rate

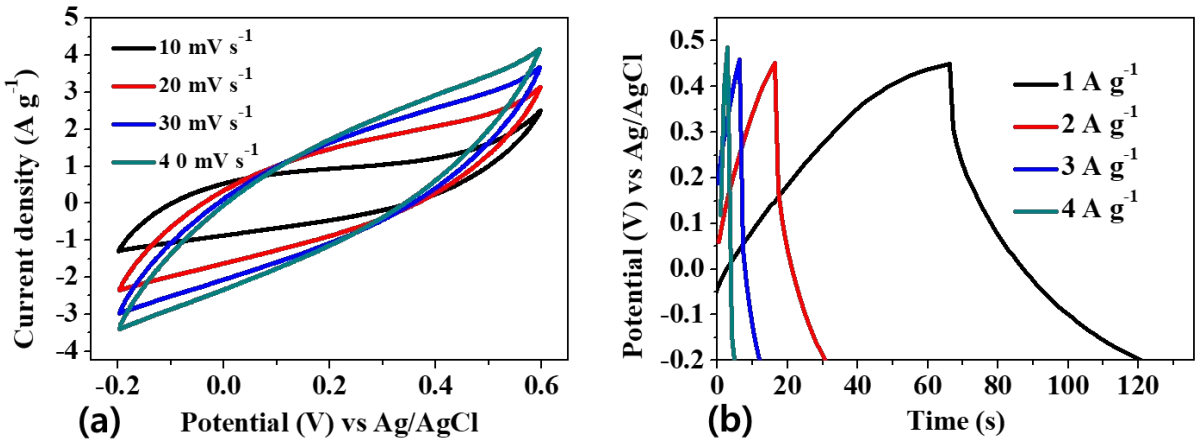

Fig. S8 Electrochemical data of as-prepared HCNFs in the range to that of 3D Co_3O_4/C@HCNFs; (a) CV curves and (b) GCD curves

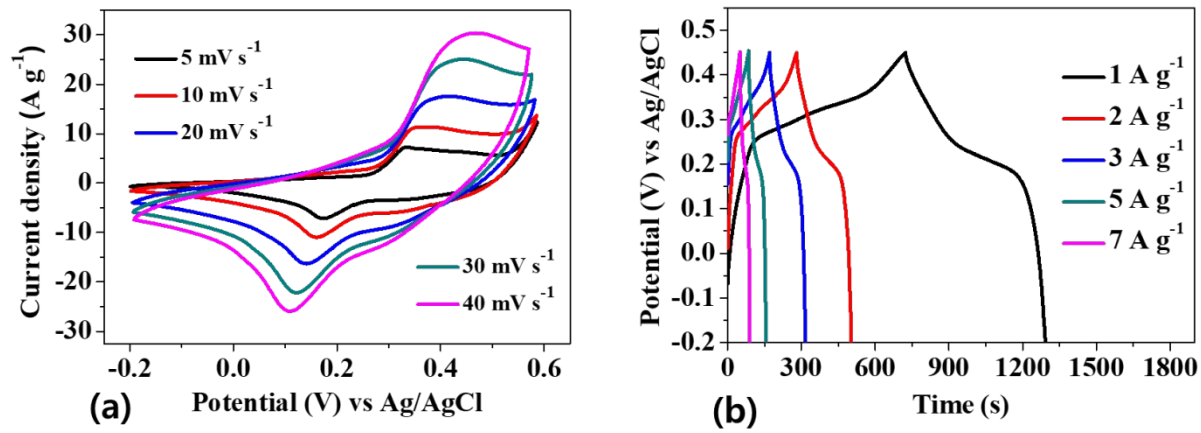

Fig. S9 Electrochemical data of as-prepared Co_3O_4/C after deposition on Ni foam; (a) CV curves and (b) GCD curves

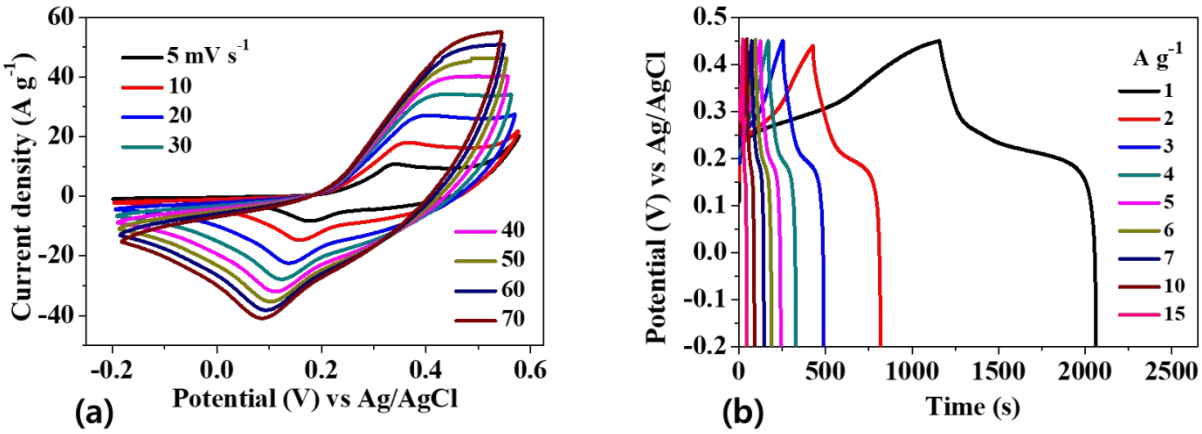

Fig. S10 Electrochemical performance of 3D Co_3O_4@HCNFs nanocomposite; (a) CV curves and (b) GCD curves

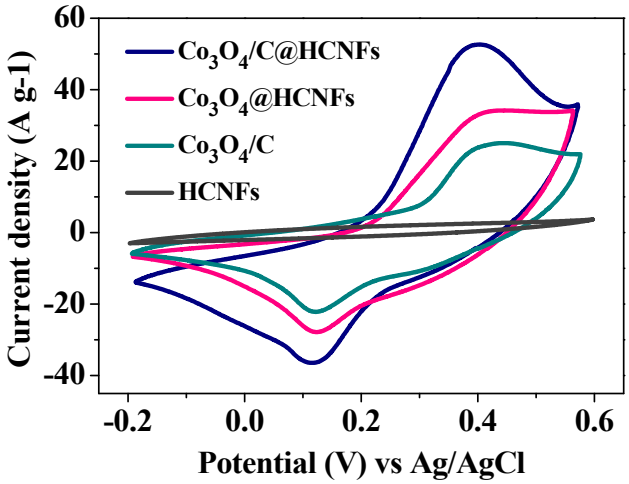

Fig. S11 Comparative CV curves at 30 mV s^{-1}

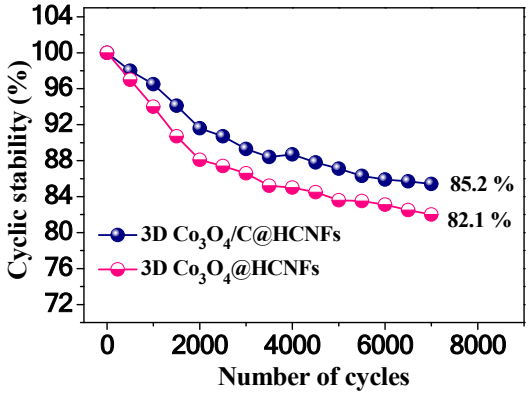

Fig. S12 Cyclic stability performance at 7 A g^{-1}

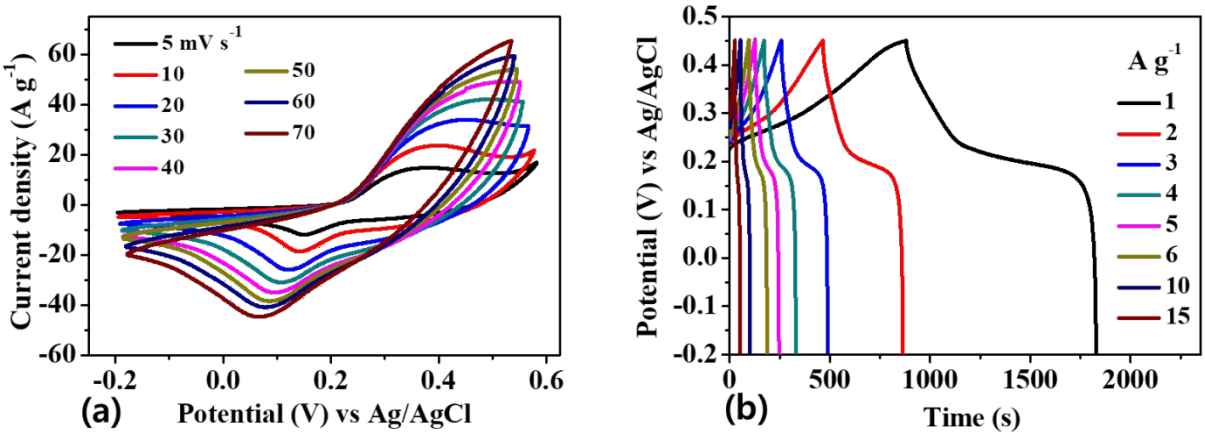

Fig. S13 Electrochemical performance of 3D Co_3O_4/C@HCNFs-35 nanocomposite; (a) CV curves and (b) GCD curves

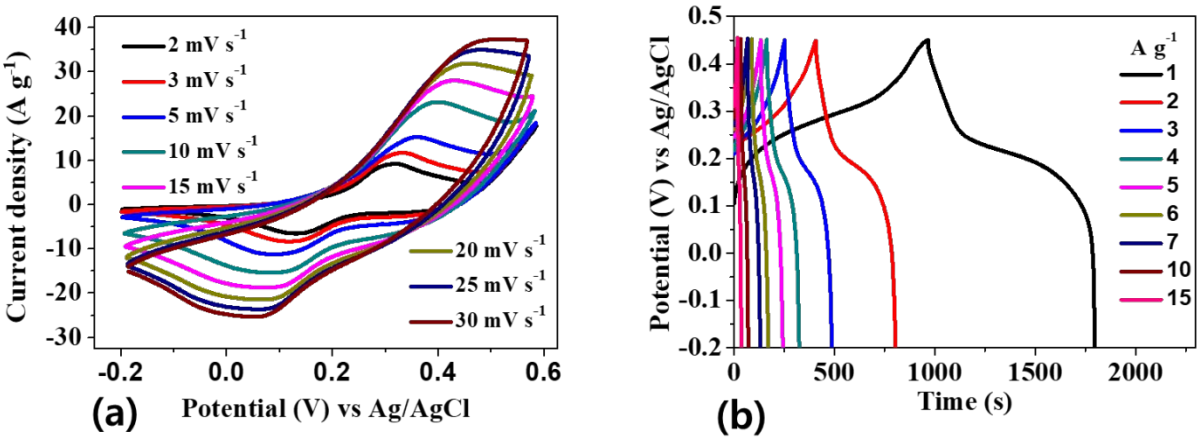

Fig. S14 Electrochemical performance of 3D Co_3O_4/C@HCNFs-70 nanocomposite; (a) CV curves and (b) GCD curves

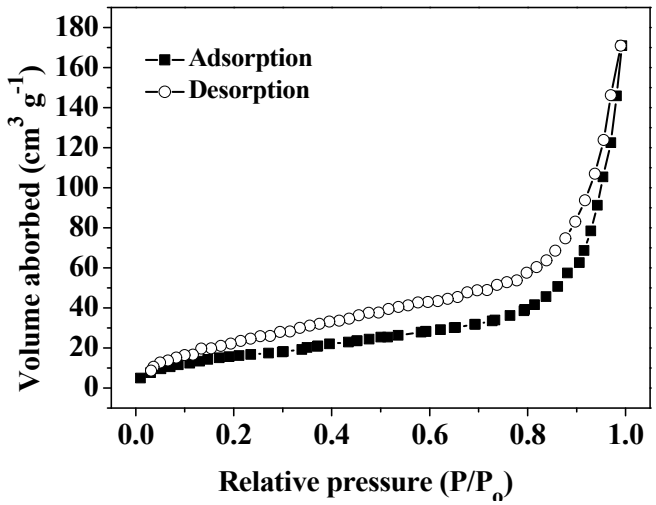

Fig. S15 N_2 adsorption-desorption isotherm of 3D Co_3O_4/C@HCNFs-35

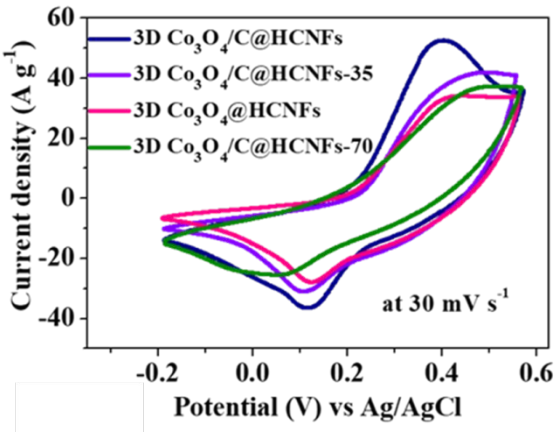

Fig. S16 Comparative CV curves

Synthesis of nitrogen-doped graphene hydrogel: Nitrogen-doped graphene hydrogel (NGH) was prepared by reported method.[1] Briefly, 30 mg of graphene oxide (GO) was dispersed in 30 ml DI water by sonication for about 15 min. 900 mg of urea was dissolved in 10 g of DI water and it was added into the GO suspension drop by drop with constant stirring. After stirring for about 30 min, it was subjected to hydrothermal process in 50 mL Teflon vessel at 160 °C for 3 h. The hydrogel formed was taken out, washed with DI water to remove excess urea and freeze-dried for 24 h.

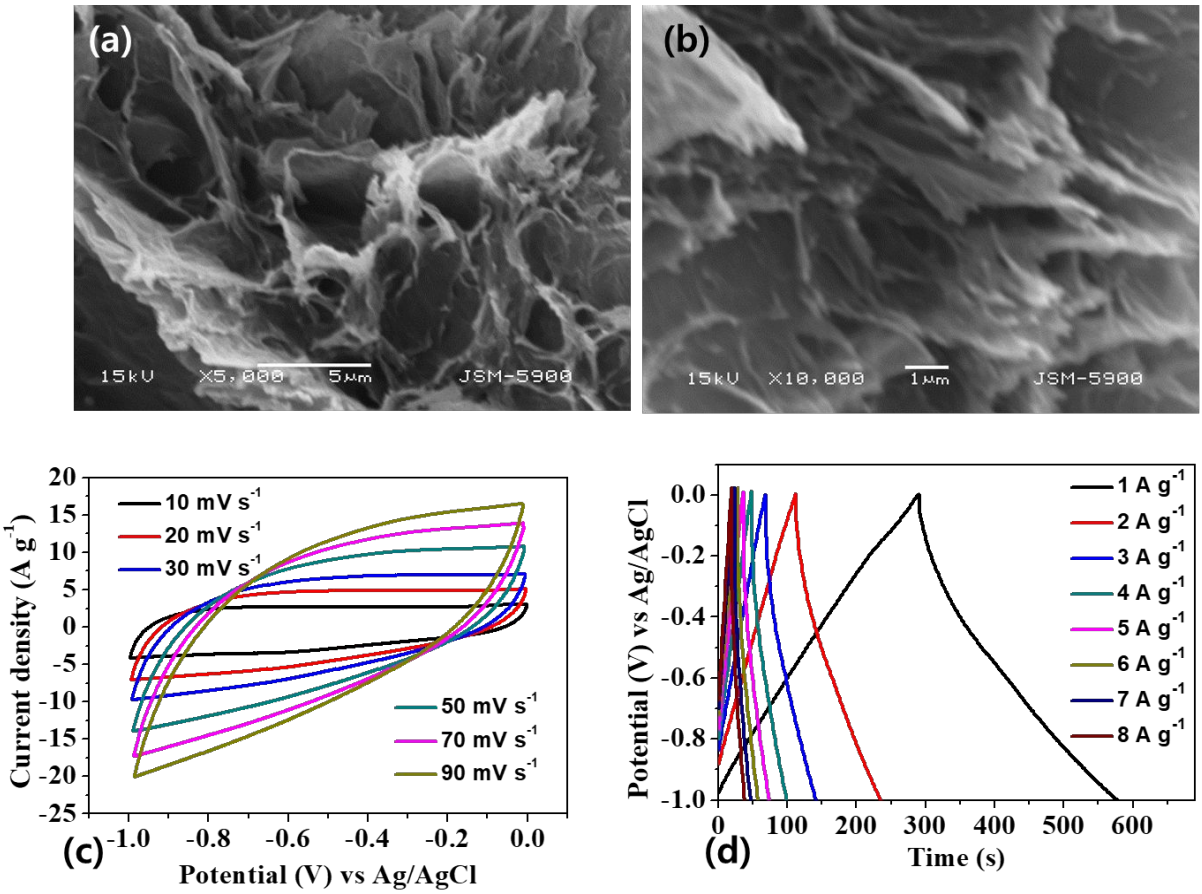

Fig. S17 NGH; (a and b) SEM images, (c) CV curves and (d) GCD curves

Based on GCD curve, as-prepared NGH exhibits specific capacity of 94 mA h g^{-1} (287 F g^{-1}) at 1 A g^{-1}.

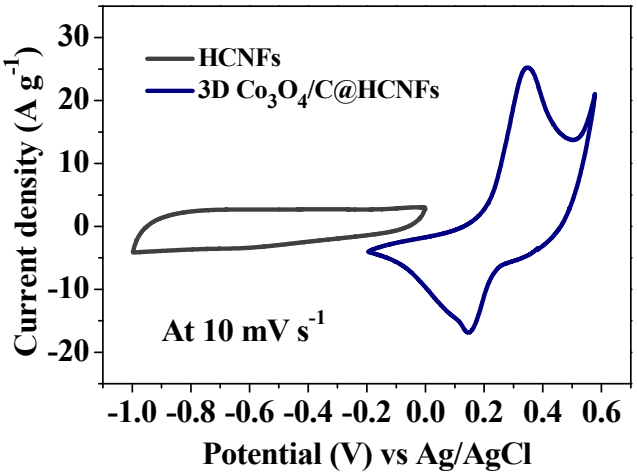

Fig. S18 Comparison of CV curves of NGH and 3D Co_3O_4/C@HCNFs measured in a three-electrode electrochemical cell

For the ASC device, the optimal mass ratio of the electrode materials were calculated using equation (2);

$$\boldsymbol{m}_{-} = \frac{\boldsymbol{C}_{+} \times \boldsymbol{V}_{+}}{\boldsymbol{C}_{-} \times \boldsymbol{V}_{-}} \times \boldsymbol{m}_{+}, \quad = \frac{\mathbf{199 \times 0.65}}{\mathbf{94 \times 1}} \times 0.004, \quad = \ 0.0051$$

Therefore, mass ratio of positive to negative electrode materials is $(\boldsymbol{m_+ : m_-})$ =1:1.3

Fabrication of asymmetric supercapacitor (ASC) device: A sheet of as-prepared 3D Co_3O_4/C@HCNFs nanocomposite was used as a positive electrode. Calculated weight of NGH was used to prepare negative electrode. A mixture of 80% NGH, 10% acetylene black and 10% poly(vinylenedifluoride) were intimately mixed in N-methyl-2-pyrrolidinone (NMP, showa) to form a homogeneous slurry. The obtained slurry was coated onto freshly cleaned and dried nickel foam, dried at 60 °C for about 8 h. Electrodes were assembled into a coin cell device using a paper separator (NKK, Nippon, Kodoshi Corporation). Before assembling into ASC coin cell device, the separator and the electrodes were soaked into 2 M aqueous KOH electrolyte.

Table S1. Elemental composition of 3D Co_3O_4/C@HCNFs nanocomposite as obtained by its XPS survey scan

Element	C 1s	O 1s	Co 2p
Atomic %	27.83	47.71	24.46

Table S2. BET surface area of as-prepared materials

Material	BET surface area (m^2 g^{-1})	Pore volume (cm^3 g^{-1})
3D Co_3O_4@HCNFs	89.1	0.22317
3D Co_3O_4/C@HCNFs	225.7	0.46531
3D Co_3O_4/C@HCNFs-35	137.2	-

Table S3. Performance of some of the recently published Co_3O_4 based materials for supercapacitors

SN	Material	Specific capacitance	Cyclic stability	Published year	Ref
1	Co_3O_4 polyhedra/rGO	1187.4 F g^{-1} at 10 mV s^{-1}		2019	[2]
2	Co_3O_4@PDA	1183 F g^{-1} at 1 A g^{-1}	-	2019	[3]
3	Co_3O_4/C	875.6 F g^{-1} at 1 A g^{-1}	87.8 % after 1000 cycles	2019	[4]
4	Co_3O_4@MCS	1409.5 F g^{-1} at 0.5 A g^{-1}	93.2 % after 1000 cycles	2019	[5]
5	Co_3O_4@$NiCo_2O_4$	879.4 F g^{-1} at 10 A g^{-1}	81.2 % after 3000 cycles	2019	[6]
6	Co_3O_4/Ni	1230.6 F g^{-1} at 1 A g^{-1}	95 % after 5000 cycles	2019	[7]
7	Mn@Co_3O_4	909 F g^{-1} at 1 A g^{-1}	71.2 % after 5000 cycles	2019	[8]
8	Co_3O_4-NiO/GF	766 F g^{-1} at 1 A g^{-1}	86 % after 5000 cycles	2019	[9]
9	Co_3O_4-SnO@SnO_2	705 F g^{-1} at 0.5 A g^{-1}	91.5 % after 2000 cycles	2019	[10]
10	Co_3O_4 nanospheres	837.7 F g^{-1} at 1 A g^{-1}	87 % after 2000 cycles	2019	[11]
11	Mn doped Co_3O_4	668.4 F g^{-1} at 1 A g^{-1}	104 % after 10000 cycles	2019	[12]
12	NiO/Co_3O_4@Graphene	1361 F g^{-1} at 1 A g^{-1}	76.4 % after 5000 cycles	2019	[13]
13	Co_3O_4/Carbon Areogel	298.9 F g^{-1} at 0.5 A g^{-1}	82 % after 1000 cycles	2019	[14]
14	Co_3O_4-G>N-PEGm	1625.6 F g^{-1} at 0.5 A g^{-1}	87 % after 5000 cycles	2018	[15]
15	Co_3O_4/NPC	885 F g^{-1} at 2.5 A g^{-1}	94 % after 10000 cycles	2018	[16]
16	Co_3O_4/3D NG/MWCNTs	2039.4 F g^{-1} at 1 A g^{-1}	94 % after 6000 cycles	2017	[17]
17	**3D Co_3O_4/C@HCNFs**	**199 mA h g^{-1} (1623 F g^{-1}) at 1 A g^{-1}**	**85.2 % after 7000 cycles**		**This work**

Table S4. Summary of some of the recently published Co_3O_4 based ASC devices

ASC device	Electrolyte	Device window (V)	Energy density (W h kg^{-1})	Power density (W kg^{-1})	Cyclic stability	Ref.
Co_3O_4@$NiCo_2O_4$//AC	1 M KOH	1.7	36	852	89.5 % after 10000 cycles	[18]
RGO/HSP-Co_3O_4//GFRGO	2 M KOH	1.7	51	800	92.3 % after 10000 cycles	[19]
Co_3O_4/$Co(OH)_2$//MPRGO	1 M KOH	1.4	37.6	4700	91% after 5000 cycles	[20]
Co_3O_4-rGO/NF//AC	1 M KOH	1.6	20	1200	94.5% after 10000 cycles	[21]
Fe_2O_3//Co_3O_4@Au@CuO	1M Na_2SO_4	1.4	33.8	40400	100 % after 10000 cycles	[22]
3D $CoWO_4$/Co_3O_4//PC	PVA-KOH	1.5	45.6	750	90.5 % after 5000 cycles	[23]
ZnO/Co_3O_4//AC	1 M KOH	1.6	47.7	7500	83 % after 5000 cycles	[24]
Co_3O_4//AC	2 M KOH	1.6	46.5	790.7	86.4 % after 8000 cycles	[25]
Co_3O_4/NHCS//AC	2 M KOH	1.5	34.5	753	84.4 % after 5000 cycles	[26]
Co_3O_4/$Ni(OH)_2$//RGO	6 M KOH	1.6	41.90	36.10	100 % after 11000 cycles	[27]
Co_3O_4-NS-H//AC	2 M KOH	1.6	134	1111	80 % after 800 cycles	[28]
$CoWO_4$/Co_3O_4//AC	3 M KOH	1.5	57.8	750	85.9 % after 5000 cycles	[29]
Co_3O_4/PANI NCs//AC	6 M KOH	1.6	41.5	800	83.4 % after 5000 cycles	[30]
Co_3O_4/ZnO//AC	6 M KOH	1.4	43.2	1401	-	[31]
$NiCo_2O_4$/ZnO/Co_3O_4 //AC	2 M KOH	1.6	83.11	8006.8	33.4 % after 3000 cycles	[32]
Co_3O_4PANI@ZIF8NC//ZIF8NC	3 M KOH	1.5	52.1	751.5	88.4 % after 10000 cycles	[33]
v-Co_3O_4/CC//NC	PVA-KOH	1.6	45.5	16300	84.5 % after 5000 cycles	[34]
3D Co_3O_4/C@HCNFs//NGH	**2 M KOH**	**1.6**	**36.6**	**471**	**85.4 % after 7000 cycles**	This work

References

1. Guo, H.-L.; Su, P.; Kang, X.; Ning, S.-K., Synthesis and characterization of nitrogen-doped graphene hydrogels by hydrothermal route with urea as reducing-doping agents. *Journal of Materials Chemistry A* **2013,** *1* (6), 2248-2255.

2. Lin, G.; Jiang, Y.; He, C.; Huang, Z.; Zhang, X.; Yang, Y., In situ encapsulation of Co_3O_4 polyhedra in graphene sheets for high-capacitance supercapacitors. *Dalton Transactions* **2019,** *48* (17), 5773-5778.

3. Zhang, X.; Zhang, R.; Xiang, C.; Liu, Y.; Zou, Y.; Chu, H.; Qiu, S.; Xu, F.; Sun, L., Polydopamine-assisted formation of Co_3O_4-nanocube-anchored reduced graphene oxide composite for high-performance supercapacitors. *Ceramics International* **2019,** *45* (11), 13894-13902.

4. Guo, S.; Xu, X.; Liu, J.; Zhang, Q.; Wang, H., Cohesive Porous Co_3O_4/C Composite Derived from Zeolitic Imidazole Framework-67 (ZIF-67) Single-Source Precursor as Supercapacitor Electrode. *Journal of The Electrochemical Society* **2019,** *166* (6), A960-A967.

5. Han, X.; Liu, S.; Shi, L.; Li, S.; Li, Y.; Wang, Y.; Chen, W.; Zhao, X.; Zhao, Y., ZIF-derived wrinkled Co_3O_4 polyhedra supported on 3D macroporous carbon sponge for supercapacitor electrode. *Ceramics International* **2019,** *45* (12), 14634-14641.

6. Zhu, Y.-R.; Peng, P.-P.; Wu, J.-Z.; Yi, T.-F.; Xie, Y.; Luo, S., Co_3O_4@$NiCo_2O_4$ microsphere as electrode materials for high-performance supercapacitors. *Solid State Ionics* **2019,** *336*, 110-119.

7. Wang, X.; Song, K.; Yang, R.; Li, J.; Jing, X.; Jun, W., Facile synthesis of nanowire and rectangular flakes of Co_3O_4 onto Ni foam for high-performance asymmetric supercapacitors. *Ionics* **2019,** *25*.

8. Chen, H.; Wang, J.; Liao, F.; Han, X.; Xu, C.; Zhang, Y., Facile synthesis of porous Mn-doped Co_3O_4 oblique prisms as an electrode material with remarkable pseudocapacitance. *Ceramics International* **2019,** *45* (6), 8008-8016.

9. Wang, P.; Zhou, H.; Meng, C.; Wang, Z.; Akhtar, K.; Yuan, A., Cyanometallic framework-derived hierarchical Co_3O_4-NiO/graphene foam as high-performance binder-free electrodes for supercapacitors. *Chemical Engineering Journal* **2019,** *369*, 57-63.

10. Wang, Z.; Long, Y.; Cao, D.; Han, D.; Gu, F., A high-performance flexible supercapacitor based on hierarchical Co_3O_4-SnO@SnO_2 nanostructures. *Electrochimica Acta* **2019,** *307*, 341-350.

11. Liu, Z.; Zhou, W.; Wang, S.; Du, W.; Zhang, H.; Ding, C.; Du, Y.; Zhu, L., Facile synthesis of homogeneous core-shell Co_3O_4 mesoporous nanospheres as high performance electrode materials for supercapacitor. *Journal of Alloys and Compounds* **2019,** *774*, 137-144.

12. Li, G.; Chen, M.; Ouyang, Y.; Yao, D.; Lu, L.; Wang, L.; Xia, X.; Lei, W.; Chen, S.-M.; Mandler, D.; Hao, Q., Manganese doped Co_3O_4 mesoporous nanoneedle array for long cycle-stable supercapacitors. *Applied Surface Science* **2019,** *469*, 941-950.

13. Yin, X.; Zhi, C.; Sun, W.; Lv, L.-P.; Wang, Y., Multilayer NiO@Co_3O_4@graphene quantum dots hollow spheres for high-performance lithium-ion batteries and supercapacitors. *Journal of Materials Chemistry A* **2019,** *7* (13), 7800-7814.

14. Wang, M.-X.; Zhang, J.; Fan, H.-L.; Liu, B.-X.; Yi, X.-B.; Wang, J.-Q., ZIF-67 derived Co_3O_4/carbon aerogel composite for supercapacitor electrodes. *New Journal of Chemistry* **2019,** *43* (15), 5666-5669.

15. Lai, C.; Sun, Y.; Zhang, X.; Yang, H.; Lin, B., High-performance double ion-buffering reservoirs of asymmetric supercapacitors based on flower-like Co_3O_4-G>N-PEGm microspheres and 3D rGO-CNT>N-PEGm aerogels. *Nanoscale* **2018,** *10* (36), 17293-17303.

16. Haldorai, Y.; Choe, S. R.; Huh, Y. S.; Han, Y.-K., Metal-organic framework derived nanoporous carbon/Co_3O_4 composite electrode as a sensing platform for the determination of glucose and high-performance supercapacitor. *Carbon* **2018,** *127*, 366-373.

17. Zhang, M.; Wang, Y.; Pan, D.; Li, Y.; Yan, Z.; Xie, J., Nitrogen-Doped 3D Graphene/MWNTs Nanoframework-Embedded Co_3O_4 for High Electrochemical Performance Supercapacitors. *ACS Sustainable Chemistry & Engineering* **2017,** *5* (6), 5099-5107.

18. Tao, K.; Yang, Y.; Yang, C.; Ma, Q.; Han, L., Construction of $NiCo_2O_4$ nanosheet-decorated leaf-like Co_3O_4 nanoarrays from metal–organic framework for high-performance hybrid supercapacitors. *Dalton Transactions* **2019,** *48* (37), 14156-14163.

19. Huang, J.; Xiao, Y.; Peng, Z.; Xu, Y.; Li, L.; Tan, L.; Yuan, K.; Chen, Y., Co3O4 Supraparticle-Based Bubble Nanofiber and Bubble Nanosheet with Remarkable Electrochemical Performance. *Advanced Science* **2019,** *6* (12), 1900107.

20. Lee, G.; Jang, J., High-performance hybrid supercapacitors based on novel Co_3O_4/$Co(OH)_2$ hybrids synthesized with various-sized metal-organic framework templates. *Journal of Power Sources* **2019,** *423*, 115-124.

21. Raj, S.; Srivastava, S. K.; Kar, P.; Roy, P., In situ growth of Co_3O_4 nanoflakes on reduced graphene oxide-wrapped Ni-foam as high performance asymmetric supercapacitor. *Electrochimica Acta* **2019,** *302*, 327-337.

22. Singh, A. K.; Sarkar, D., Substrate-integrated core–shell Co_3O_4@Au@CuO hybrid nanowires as efficient cathode materials for high-performance asymmetric supercapacitors with excellent cycle life. *Journal of Materials Chemistry A* **2017,** *5* (41), 21715-21725.

23. Zhang, M.; Fan, H.; Ren, X.; Zhao, N.; Peng, H.; Wang, C.; Wu, X.; Dong, G.; Long, C.; Wang, W.; Gao, Y.; Ma, L.; Wu, P.; Li, H.; Jiang, X., Study of pseudocapacitive contribution to superior energy storage of 3D heterostructure $CoWO_4$/Co_3O_4 nanocone arrays. *Journal of Power Sources* **2019,** *418*, 202-210.

24. Gao, M.; Wang, W.-K.; Rong, Q.; Jiang, J.; Zhang, Y.-J.; Yu, H.-Q., Porous ZnO-Coated Co_3O_4 Nanorod as a High-Energy-Density Supercapacitor Material. *ACS Applied Materials & Interfaces* **2018,** *10* (27), 23163-23173.

25. Wei, G.; Zhou, Z.; Zhao, X.; Zhang, W.; An, C., Ultrathin Metal–Organic Framework Nanosheet-Derived Ultrathin Co_3O_4 Nanomeshes with Robust Oxygen-Evolving Performance and Asymmetric Supercapacitors. *ACS Applied Materials & Interfaces* **2018,** *10* (28), 23721-23730.

26. Liu, T.; Zhang, L.; You, W.; Yu, J., Core–Shell Nitrogen-Doped Carbon Hollow Spheres/Co_3O_4 Nanosheets as Advanced Electrode for High-Performance Supercapacitor. *Small* **2018,** *14* (12), 1702407.

27. Tang, C.-h.; Yin, X.; Gong, H., Superior Performance Asymmetric Supercapacitors Based on a Directly Grown Commercial Mass 3D Co_3O_4@$Ni(OH)_2$ Core–Shell Electrode. *ACS Applied Materials & Interfaces* **2013,** *5* (21), 10574-10582.

28. Yang, Q.; Lu, Z.; Sun, X.; Liu, J., Ultrathin Co_3O_4 nanosheet arrays with high supercapacitive performance. *Scientific Reports* **2013,** *3*, 3537.

29. Zhang, M.; Fan, H.; Zhao, N.; Peng, H.; Ren, X.; Wang, W.; Li, H.; Chen, G.; Zhu, Y.; Jiang, X.; Wu, P., 3D hierarchical $CoWO_4$/Co_3O_4 nanowire arrays for asymmetric supercapacitors with high energy density. *Chemical Engineering Journal* **2018,** *347*, 291-300.

30. Ren, X.; Fan, H.; Ma, J.; Wang, C.; Zhang, M.; Zhao, N., Hierarchical Co_3O_4/PANI hollow nanocages: Synthesis and application for electrode materials of supercapacitors. *Applied Surface Science* **2018,** *441*, 194-203.

31. Xu, J.; Liu, S.; Liu, Y., Co_3O_4/ZnO nanoheterostructure derived from core–shell ZIF-8@ZIF-67 for supercapacitors. *RSC Advances* **2016,** *6* (57), 52137-52142.

32. Zhou, S.; Hao, C.; Wang, J.; Wang, X.; Gao, H., Metal-organic framework templated synthesis of porous $NiCo_2O_4$/$ZnCo_2O_4$/Co_3O_4 hollow polyhedral nanocages and their enhanced pseudocapacitive properties. *Chemical Engineering Journal* **2018,** *351*, 74-84.

33. Chhetri, K.; Tiwari, A.; Dahal, B.; Ojha, G.; Lee, M.; Kim, T.; Chae, S.-H.; Muthurasu, A.; Kim, H., A ZIF-8-derived nanoporous carbon nanocomposite wrapped with Co_3O_4-polyaniline as an efficient electrode material for an asymmetric supercapacitor. *Journal of Electroanalytical Chemistry* **2019**, 113670.

34. Dai, S.; Han, F.; Tang, J.; Tang, W., MOF-derived Co_3O_4 nanosheets rich in oxygen vacancies for efficient all-solid-state symmetric supercapacitors. *Electrochimica Acta* **2019,** *328*, 135103.